DIAGNOSIS DESIGN OF SHIP HULL STRENGTH OF TREATED BY DYNAMIC LOAD

Andrzej GRZĄDZIELA[1], Bogdan SZTUROMSKI[2], Marcin KLUCZYK[3]

Polish Naval Academy, Mechanical Department, 81-103 Gdynia, Śmidowicza St. 69, Poland
[1]a.grzadziela@amw.gdynia.pl, [2]B.Szturomski@amw.gdynia.pl, [3]M.Kluczyk@amw.gdynia.pl

Summary

Ship shock tests have been conducted for shock qualification of hull integrity and proper operation systems and subsystems. The ship shock trial identifies design and construction and it also validates shock hardening criteria. The main problem is that ship shock trials are costly. Numerical modeling and simulation, using FEM, may provide information to look into the details of fluid model, dynamic characteristics of ship hull and its internal component. The ship shock modeling and simulation has been performed and the predicted results were compared with ship shock test data made into sea trials. The preliminary studies of shock analysis approach are presented and the important parameters are discussed.

Keywords: simulation, underwater explosion, minehunter, hull

DIAGNOZOWANIE PROJEKTOWE WYTRZYMAŁOŚCI KADŁUBA OKRĘTOWEGO PODDANEGO ODDZIAŁYWANIOM DYNAMICZNYM

Streszczenie

Testy udarnościowe kadłubów prowadzone są w celu oceny ich integralności oraz poprawności działania wszystkich zamontowanych systemów. Testy udarnościowe pozwalają na identyfikację i ocenę konstrukcji oraz weryfikują odporność kadłuba. Głównym problemem jest ich wysoka cena z racji konieczności realizacji na prototypach. Modelowanie i symulacja za użyciem MES, może dostarczyć informacji do oceny bryły wody towarzyszącej, dynamicznych właściwości kadłuba i elementów wyposażenia. W artykule przedstawiono modelowanie i symulację uderzenia w fali uderzeniowej w kadłub a uzykane wyniki porównano z wynikami poligonowymi.

Słowa kluczowe: symulacja, wybuchy podwodne, niszyciele min, kadłub

1. INTRODUCTION

Large capacity of the calculating hardware help to make assessments of short-term (fast changing) processes, such as the impact of the pressure wave from a no-contact underwater explosion near the hull of the ship. These are issues of great complexity and indirection, each should be treated individually. It is necessary to simplify the task in many areas, because too accurate descriptions of the phenomenon may give results far from the actual one. The task becomes much more complicated in case of including the interaction between the environment and the contemplated construction. The ship is located in two mediums: water and air. Taking into account the impact of these requires solving the double-linked task using for example the finite element and boundary element method. Then the solution, at the edge of a particular medium, eg. liquid, forms the input data for the load of the deformed structure impacting on the surrounding medium. Such mutual linkage is repeated n times and at every step of the data exchange it is necessary to obtain adequate convergence. The problem becomes more complicated due to numerous non-linearity. In the case of the impact loads by pressure wave it is not possible to disregard large displacement structures, nonlinearity of materials, failure criteria, etc. In the case of complex structures there will be contact. All these factors determine the complexity of the task and the processing power needed to obtain solutions in a reasonable time, with the possibility of assessing its results, making any corrections and repeating the calculations.

2. THE DYNAMIC EQUATION OF MOTION IN TERMS OF MES – EXPLICITE

To determine the motion parameters of the discrete model consisting of a finite number of elements in the MES the differential equation of the form [1] must be solved:

$$\mathbf{M}\ddot{U} + \mathbf{C}\dot{U} + \mathbf{K}U = F \qquad (1)$$

where:
$\mathbf{K}$ - the stiffness matrix of the structure;
$\mathbf{M}$ - matrix of inertia;
$\mathbf{C}$ - matrix of damping;
$U, \dot{U}, \ddot{U}$ - the vector of displacement, velocity and acceleration;

F - the vector of loads.

Stiffness matrix **K** reflects the material properties of the element and geometry. In MES stiffness matrix $\mathbf{K^e}$ for the element is defined as the product of the elasticity and deformation matrices in the form [2]:

$$\mathbf{K^e} = \int_V \mathbf{B}^T \mathbf{D} \, \mathbf{B} \, \mathrm{d}V \qquad (2)$$

where:
B - matrix deformation element;
D - matrix element of elasticity;
V - volume element.

Inertia matrix **M** - reflects the mass and the mass moments of inertia, is created the same way for the entire structure as the structure stiffness matrix **K**. The MES inertia matrix $\mathbf{M^e}$ for the item is defined as a square shape functions [2]:

$$\mathbf{M}^e = \rho \int_V \mathbf{N^T N} \, dV \qquad (3)$$

where:
N - matrix of shape functions;
ρ - density of the element;
V - volume element.

C is the damping matrix. Most define it as a linear combination of the inertia matrix and stiffness matrix [2]:

$$\mathbf{C} = \alpha \mathbf{M} + \beta \mathbf{K} \qquad (4)$$

Where α and β are constant coefficients, which determine the manner specified in [3]. U represents the vector of generalized displacement of the nodes, whereas their derivatives over time represent velocity and acceleration of nodes, F is the vector of external nodal forces. These matrices and vectors in a given task depend on the type of finite elements used to describe the area in question, which translates into the size of the task. In these types of issues, reflecting the geometry of the study area and its discretization acquire a completely different dimension, as their depend on the size of the task, the computation time and the results obtained. The equation of motion with specified initial conditions at time t_0 is the basic system of equations:

$$U(t_0) = U_0 \quad \dot{U}(t_0) = \dot{U}_0 \qquad (5)$$

The CAE program includes a number of ways of integration of equations of motion [1, 3, 4, 5]. The most popular are the so-called direct methods, also called step-by-step methods, or simply dynamic explicit. They are applied to any equations untreated by transformation. They are based on the assumption that the equation is satisfied in certain moments of time t_0, $t_0+\Delta t$, $t_0+2\Delta t$, ... , t_1, and not the entire time interval $\langle t_0, \quad t_1\rangle$. The nature of variation, displacement, velocity and acceleration are assumed during the relevant time period $\langle t, \quad t+\Delta t\rangle$. With these assumptions, the integration algorithm is reduced to finding a solution at time $t_0+i\Delta t$ by using the known

values of the function in the moments preceding t_0, $t_0+\Delta t$, $t_0+2\Delta t$, $t_0+(i-1)\Delta t$. The most common methods of numerical integration of equations of motion are: Euler's, Newmark's and Wilson's [1, 2, 3, 4]. In Newmark's numerical integration method, the basic formulas are given by [1]:

$$U_{t+\Delta t} = U_t + \dot{U}_t \Delta t + \left[\left(\frac{1}{2} - \beta \right) \ddot{U}_t + \beta \, \ddot{U}_{t+\Delta t} \right] (\Delta t)^2$$

$$\dot{U}_{t+\Delta t} = \dot{U}_t + \left[(1+\gamma) \ddot{U}_t + \gamma \, \ddot{U}_{t+\Delta t} \right] \Delta t \qquad (6)$$

where β, γ are constant factors affecting the stability and accuracy of the method. It was shown that for the values $\beta = 0,25$ and $\gamma = 0,5$ the method is unconditionally stable in papers [1,3]. Solving equations (1 and 5) with respect to $\dot{U}_{t+\Delta t}$ and $\ddot{U}_{t+\Delta t}$ we obtain:

$$\ddot{U}_{t+\Delta t} = \frac{1}{\beta \, (\Delta t)^2} \left[U_{t+\Delta t} - U_t - \dot{U}_t \Delta t + (\Delta t)^2 \left(\beta - \frac{1}{2} \right) \ddot{U}_t \right]$$

$$(7)$$

$$\dot{U}_{t+\Delta t} = \frac{\gamma}{\beta \, \Delta t} (U_{t+\Delta t} - U_t) + \left(1 - \frac{\gamma}{\beta} \right) \dot{U}_t + \left(1 - \frac{\gamma}{2\beta} \right) \Delta t \, \ddot{U}_t$$

Substituting vectors (7) to the equations of motion (1) gives the algebraic equation in the form:

$$\left[\frac{1}{\beta \, (\Delta t)^2} \mathbf{M} + \frac{\gamma}{\beta \, \Delta t} \mathbf{C} + \mathbf{K} \right] U_{t+\Delta t} =$$

$$= F_{t+\Delta t} + \mathbf{M} \left[\frac{1}{\beta \, (\Delta t)^2} U_t + \frac{1}{\beta \, \Delta t} \dot{U}_t + \left(\frac{1}{2\beta} - 1 \right) \ddot{U}_t + \right] \qquad (8)$$

$$+ \mathbf{C} \left[\frac{\gamma}{\beta \, \Delta t} U_t + \left(\frac{\gamma}{\beta} - 1 \right) \dot{U}_t + \Delta t \left(\frac{\gamma}{2\beta} - 1 \right) \ddot{U}_t \right]$$

From the above equation displacement vector $U_{t+\Delta t}$ can be calculated. Then, from equations (7) the velocity and acceleration vectors $\dot{U}_{t+\Delta t}$ and $\ddot{U}_{t+\Delta t}$ can be obtained. Repeating this procedure for successive moments we obtain a solution in the considered time interval $\langle t_0, t_1 \rangle$.

Substituting $\beta=1/4$ and $\gamma=1/2$ we get the equation:

$$\left[\frac{4}{(\Delta t)^2} \mathbf{M} + \frac{2}{\Delta t} \mathbf{C} + \mathbf{K} \right] U_{t+\Delta t} =$$

$$= F_{t+\Delta t} + \mathbf{M} \left[\frac{4}{(\Delta t)^2} U_t + \frac{4}{\Delta t} \dot{U}_t + \ddot{U}_t \right] + \qquad (9)$$

$$+ \mathbf{C} \left[\frac{2}{\Delta t} U_t + \dot{U}_t \right]$$

and

$$\ddot{U}_{t+\Delta t} = \frac{4}{(\Delta t)^2} \left[U_{t+\Delta t} - U_t - \dot{U}_t \Delta t - \frac{1}{4} (\Delta t)^2 \ddot{U}_t \right] \quad (10)$$

$$\dot{U}_{t+\Delta t} = \frac{2}{\Delta t} (U_{t+\Delta t} - U_t) - \dot{U}_t$$

The above procedure is implemented in a number of commercial applications. 'Dynamic explicit' gives a fairly stable solution, even for highly nonlinear problems. When the nonlinear static analysis obtaining a solution fails, it is recommended to repeat the task in terms of 'dynamic explicit'.

3. SELECTION OF TIME STEP IN A FAST-CHANGING ISSUES

The problem in dynamic analysis is the time step size [6]. The smaller its size, the smaller the size of the used finite elements. This relationship is very unfavorable, because the grid density is associated with a reduction in the time step. For example, doubling the number of items and selecting the appropriate time step to the new dimensions of elements may longer the computation time 10-20 times. For a dense grid time step values are of the order 10^{-6} s, and even smaller. In the fast-changing processes such as loading the construction with a pressure wave from the explosion, where the duration of load is a fraction of a millisecond in a row, time step is determined by the history of the load.

Experiments show that the solution of the dynamic task is stable when the initial time step value is less than 1/10 of the first period frequency. Good results are obtained through adoption of the time step, as the ratio of the smallest dimension of the grid elements to the speed of propagation of elastic waves (acoustic) in the material element, that is:

$$\Delta t = \frac{h}{a} \qquad (11)$$

where:
h - the smallest dimension of the grid elements;

$a = \sqrt{E/\rho}$ - elastic wave velocity (acoustic).

After determining the value of time step, due to the size of the elements, one has to make sure it reflects the entire history of the load, if it should not be reduced by subsequent orders, which can lead to the range of 10^{-7}, 10^{-8} s.

4. REFLECTION OF THE GEOMETRY AND DISCRETIZATION OF THE RESEARCH

In formulating the task in terms of MES at the stage of reflecting the geometry the size of the task in relation to the computational capabilities must be taken into the account. Usually, we intend to faithfully reflect the geometry of the object. Unfortunately, the increase in accuracy will mainly increase the number of elements in the future discretization, reducing their size and the need for using solid elements of higher order. Experiments show that one should use the simplest elements possible to describe the structure. To describe the

geometry of objects such as ships it is proposed to use the shell and beam elements, and equipment constituting interior modeled as concentrated masses of the respective nodes (Fig. 1).

Figure 1. The geometry of the hull with the centered masses

The possibility of applying the masses gathered in the MES software algorithms can significantly reduce the size of the task, by reducing the number of elements to describe the geometry. In the nodes of the elements the mass moments of inertia can be attributed [7]. Thus, to include in the calculation model of the equipment, for example, the generator, it is not necessarily a reflection of its geometry, it is sufficient to determine its mass and calculate the mass inertia moments given the point of the ship structure and assign these values to that point. It is recommended to "distribute" such data on a few points. To present the problem, the shape functions for linear (4-node) shell element and linear (8-node) solid element are summarised below. Shape function for the linear 4-node element [7]:

$$u(g, h) = \frac{1}{4}(1 - g)(1 - h)u_1 +$$
$$+\frac{1}{4}(1 + g)(1 - h)u_2 +$$
$$+\frac{1}{4}(1 + g)(1 + h)u_3 + \qquad (12)$$
$$+\frac{1}{4}(1 - g)(1 + h)u_4$$

Shape function for the linear hexagonal 8-node element [7]:

$$u(g, h, r) = \frac{1}{8}(1 - g)(1 - h)(1 - r)u_1 +$$
$$+\frac{1}{8}(1 + g)(1 - h)(1 - r)u_2 +$$
$$+\frac{1}{8}(1 + g)(1 + h)(1 - r)u_3 +$$
$$+\frac{1}{8}(1 - g)(1 + h)(1 - r)u_4 + \qquad (13)$$
$$+\frac{1}{8}(1 - g)(1 - h)(1 + r)u_5 +$$
$$+\frac{1}{8}(1 + g)(1 - h)(1 + r)u_6 +$$
$$+\frac{1}{8}(1 + g)(1 + h)(1 + r)u_7 +$$
$$+\frac{1}{8}(1 - g)(1 + h)(1 + r)u_8 +$$

The geometry of the mine hunter 206FM - Fig. 2, is presented below by 14 475 square coating components, coating 76 triangular elements, set in space by 11 753 nodes, which at the 6 degrees of freedom at each node gives 70 518 degrees of freedom of the whole structure. It is also the size of the matrix **K**, **M** and **C**.
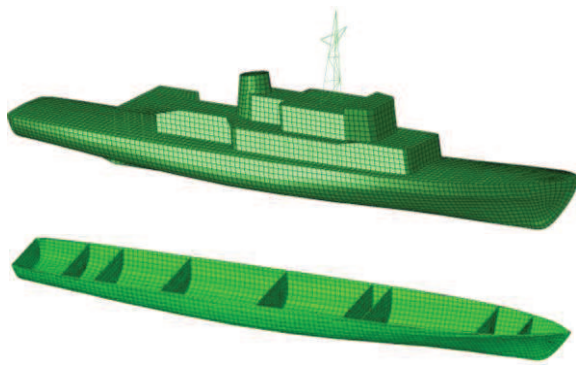
Figure 2. Polish mine hunter 206FM's
- discrete model and its cross-section

5. CONSTRUCTION LOAD – PRESSURE WAVE AFFECTING THE SHIP

Simplified descriptions of the pressure distribution as a function of time and distance from the explosion of pyrotechnic substance both in water and air are given in the literature of the twentieth century, and they can be implemented into computer programs. The explosion is the process of deflagration pressure increase that occurs in a very short time (milliseconds). The nature of this process is determined by the dynamic conditions in which the combustible mixture and, in particular turbulence medium is located. Pressure waves, called shock waves, formed during the explosion in air travel at the speed of 1000 3000 m/s and in liquid (explosion under water) or in solids reach up to 8000 m/s. Typical detonation velocity in the air range from 1500 to 3000 m/s, while the pressure reaches a value of 1 to 100 MPa. Before the arrival of the shock wave front the pressure is equal to atmospheric pressure. With the advent of the front, the pressure is rising rapidly up to a maximum value called the peak positive overpressure. Then the pressure drops to atmospheric pressure. The period of a further drop in pressure and the return to atmospheric pressure is called the period of negative phase. Important parameters of the process are: the maximum value of pressure and the area under the function describing the pressure dependence of time during the positive phase. The nature and mechanism of the explosion is determined by numerous parameters, which include:
• material properties (physical, chemical stability, heat of combustion, etc..)
• space in which combustion occurs (size, open, closed, barriers, etc.);
• properties of explosive mixtures (concentration, pressure and temperature);
• way of ignition (energy, temperature).
Here are the results of pressure measurements made on the range during the detonation of an equal mass of explosives such as hexogen (RDX), trinitrotoluene (TNT), metanite (2H), dynamite (20G5H) ammonite (54H), measured at a distance of 2 m from the burst's centre (Fig. 3). The experiment

was carried out by employees of the Department of Mining and Geo-engineering, AGH University in Krakow [9].
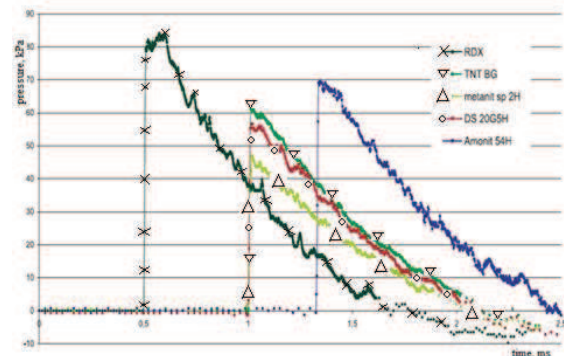

Figure 3. Pressure values at a distance
of 2 m from the centre of detonation
for various explosives (source: WGiG
AGH in Cracow) [9]

For the strength calculations simplified models of the detonation wave are assumed [8], which usually does not take into the account the vacuum phase (Fig. 4). It is important that the time step used for the calculations included the entire history of the load, because in case of a bad choice, the phase of hypertension may be extended or completely omitted.
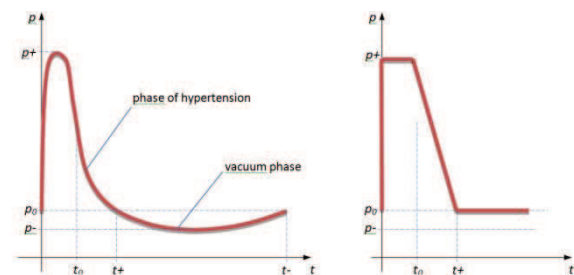

Figure 4. The structure of the shock
wave and its simplification

The TNT explosion is very well described by a perfect shock wave structure, with a rapid pressure rise, a short period of positive phase from 1 to 10 ms and hypertension to 100 MPa. In case of the closed or partially closed volume, there exist other phases of the shock wave associated with the reflection from the surrounding structures. In [9] quoted several ways to determine pressure and pulse of the pressure wave depending on the distance from the explosion and the mass of the detonated load. The type of explosive is also taken into an account. For the purposes of calculations and numerical simulations to determine the intensity of pressure on the front of the wave *p(t)* the historical, but still current dependencies are commonly used, known as Cole's model [10] of the form:

$$p_m(t) = 52.3 \left(\frac{\sqrt[3]{m}}{R} \right)^{1.13} \cdot e^C \qquad (14)$$

$$C = \frac{-t \cdot 1000}{0.093 \cdot \sqrt[3]{m}\left(\frac{\sqrt[3]{m}}{R}\right)^{-0.22}} \qquad (15)$$

where:
p_m - the pressure on the front of the wave, MPa,
t - time, s,
R - distance from the load, m,
m - mass of the load, kg.

These patterns allow the determination of the pressure at the front of the shock wave in water and in function of distance from the epicenter of detonation, the payload and the time period from the time of the wave at a given point in space (and not from the moment of detonation). Thus, to apply the above description in MES, a procedure should be prepared (including the above formulas) developed to describe the pressure distribution in space as a function of time from the moment of detonation, and taking into account the angle of incidence of waves on an item as it has a particular direction and vector features (Fig. 5) [8].
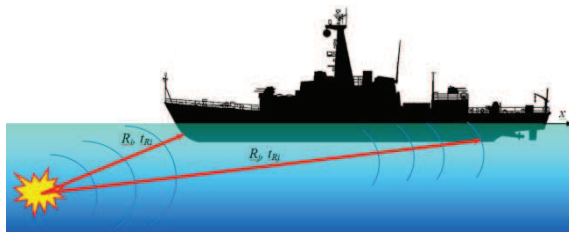

Figure 5. The distance of the element from the epicenter and the wave transit time

In this procedure, the wave transit time from the moment of explosion until you reach the first point of the structure should be omitted. This procedure was repeated for each element in a given time step. Pressure wave velocity to be used in a given medium might be a problem as it is not constant. As mentioned above, in water in the first phase of the outbreak it reaches a speed of up to 8000 m/s, then moving on, the speed drops to the speed of sound in a given medium, i.e. for water to approximately 1500 m/s. Therefore, if the epicentre of the outbreak is far enough away from the structure (over 10 m), for the calculation, it can be assumed that speed of propagation of the pressure wave is constant - equal to the speed of sound. For smaller distances it should be a description of the wave velocity as a function of distance. Ultimately, this procedure gives states the load structure at discrete moments in time. This approach can be directly implemented in CAE.
Summing up, setting the load for a particular element of construction, the time in formulas (14), must move by the value of t_R which is:

$$t_R = {R}/{v_c} \qquad (16)$$

where:
t_R - time for the pressure wave to reach the component, s

R - distance from the load to the center of the element, m
v_c - sound velocity in the medium surrounding the structure, m/s

The time interval from 0 to t_R element under consideration is not influenced. The speed of sound for sea water is 1500 m/s.
To take into account the angle of the wave for a given element (Fig. 6) it is necessary to appoint two vectors, the vector normal to the element n and the pressure wave vector R whose origin is at the epicenter of the outbreak K and which ends at the center of S.
If the shell element is determined, in space, by four nodes with coordinates:

$$
\begin{aligned}
&A\ (x_a; y_a; z_a) \\
&B\ (x_b; y_b; z_b) \\
&C\ (x_c; y_c; z_c) \\
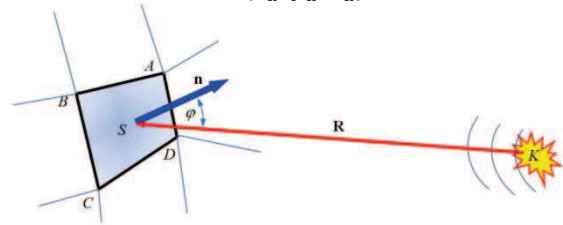&D\ (x_d; y_d; z_d)
\end{aligned} \qquad (17)
$$

Figure 6. Element influenced by the pressure wave.

The coordinates of the centre element of $S\ (x_s; y_s; z_s)$ is calculated as the mean of these coordinates:

$$
\begin{aligned}
x_s &= \frac{x_a + x_b + x_c + x_d}{4} \\
y_s &= \frac{y_a + y_b + y_c + y_d}{4} \\
z_s &= \frac{z_a + z_b + z_c + z_d}{4}
\end{aligned} \qquad (18)
$$

Assuming that the epicenter of the outbreak is at the point $K\ (x_k; y_k; z_k)$, the components of the vector R are:

$$
\begin{aligned}
R_x &= x_s - x_k \\
R_y &= y_s - y_k \\
R_z &= z_s - z_k
\end{aligned} \qquad (19)
$$

The coordinates of the normal vector n to the element in question is obtained by multiplying two vectors such as AB and CB built on the sides of elements whose components are:

$$
\begin{array}{ll}
AB_x = x_a - x_b & CB_x = x_c - x_b \\
AB_y = y_a - y_b & CB_y = y_c - y_b \\
AB_z = z_a - z_b & CB_z = z_c - z_b
\end{array} \qquad (20)
$$

Then n = AB × CB:

$$
\begin{aligned}
n_x &= AB_y \cdot CB_z - AB_z \cdot CB_y \\
\mathbf{n_y} &= \mathbf{AB_z \cdot CB_x - AB_x \cdot CB_z} \\
n_x &= AB_x \cdot CB_y - AB_y \cdot CB_x
\end{aligned} \qquad (21)
$$

Cosine of the angle φ between vectors n and R is determined from the definition of scalar product:

$$n \cdot R = |n| \cdot |R| \cdot \cos\varphi \qquad (22)$$

thus:

$$\cos\varphi = \frac{n \cdot R}{|n| \cdot |R|} == \frac{n_x \cdot R_x + n_y \cdot R_y + n_z \cdot R_z}{\sqrt{n_x^2 + n_y^2 + n_z^2} \cdot \sqrt{R_x^2 + R_y^2 + R_z^2}} \qquad (23)$$

Eventually the value of the pressure influencing the element is:

$$\text{for} \qquad t_c < t_R \Rightarrow p(t_c) = 0 \qquad (24)$$
$$\text{for} \qquad t_c \geq t_R \Rightarrow p(t_c) = $$
$$p_m(t_R + t) \cdot \cos\varphi \qquad (25)$$

In CAE, the above algorithm for determining the pressure of the item must be made in the form of the calculation procedure. For example, in Abaqus such a procedure is done in Fortran.

The following are illustrative graphs of the pressure on the hull of the mine destroyer, project 206FM, at two points: on the bow and stern. After including the speed of propagation of pressure waves in water, equal to 1500 m/s, in the case of 250 kg of TNT, detonated at a depth of 15 m with a distance of 20 meters in front, the pressure of the wave reaches the maximum value of 11 MPa and continually decreases. At the second point on the stern of the ship the pressure amounts to about 5 MPa, and it appears on the fuselage 0.035 s under the first point on the bow.
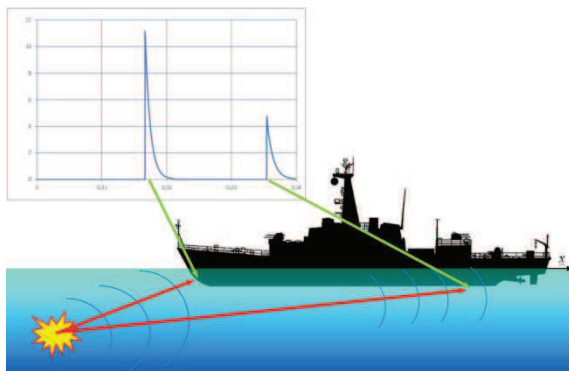

Figure **7**. Pressure at two points of the ship (detonation in the distance of 20 m in front of the ship, depth of 15 m, weight of 250 kg).

6. THE SIMULATION RESULTS ON THE EFFECTS OF UNDERWATER DETONATION OF THE SHIP HULL

Characteristics presented on the figure 8 shows simulation of the pressure at the front of detonation wave as a function of mass of the TNT load and distance from the epicenter, determined by the Cole's formula.
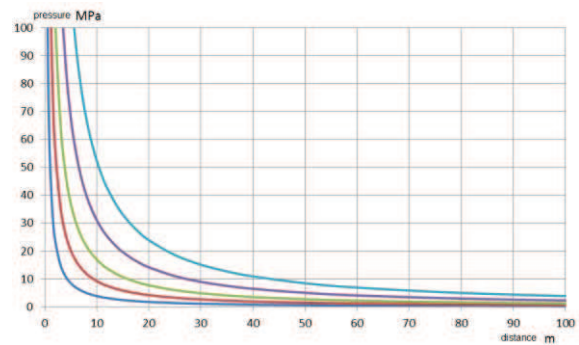

Figure 8. Pressure values at the front of the shock wave as a function of load mass of TNT of 1, 10, 50, 250, 1000 kg

Times that occur in the Cole's formulas, and is counted from the time of the wave pressures at a given point of space, does not include conveyance from the epicenter [4,6]. The pressure wave in the first phase of the explosion propagates at the speed of detonation of an estimated V = 5000 ÷ 8000 m/s. The velocity rapidly decreases to the velocity of sound in the medium [10]. After taking into account velocity of propagation of pressure waves in water of V =1500 m/s, the minehunter 206 FM type and TNT load equal mass m=250 kg, exploded at a depth of 15 m with a distance of 20 m from the bow or the stern, the pressure wave reaches the maximum value of p=11 MPa and decreases along the ship to the p=3MPa – figure 9. The total time of occurrence the load on the structure of the ship is 0.0376 s.
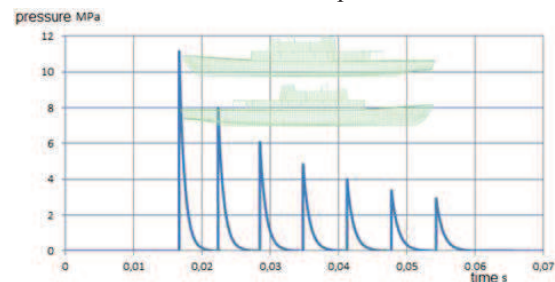

Figure 9. Pressure wave propagation along the length of the ship, detonation at a distance of 20 m before (behind) the ship.

For the same TNT load, exploded at a depth of 15 m with a distance of 20 m on the beam, the maximum shock wave pressure reaches p=11 MPa at amidships and decreases along the ship to the value of p=5.9 MPa at the bow and stern. The total time of occurrence load on the hull of the ship is more than a half shorter and equal t=0.0124 s. Distribution of pressure waves on the hull of the ship, coming from the TNT load exploded is presented on figure 10.
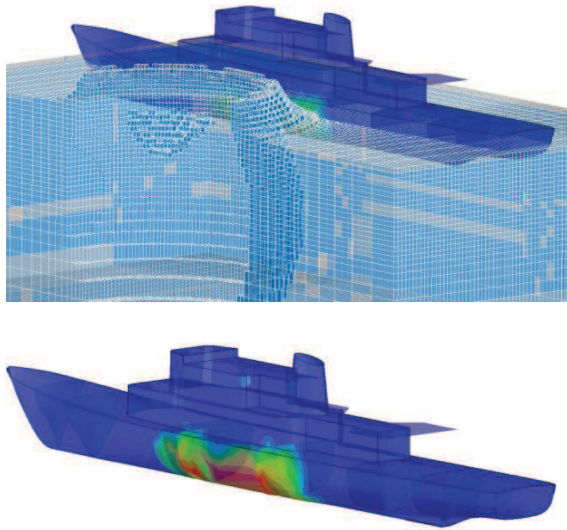
Figure 10. Distribution of shock wave
(left figure) and values of pressure
(right figure) on the hull coming from
the TNT load explosion

Pressure wave causes the hull load over its entire length. Figure 11 shows an example of the time course of the acceleration from the explosion of 250 kg TNT load at a distance of 20 m, at a depth of 15 m from the bow of the ship.
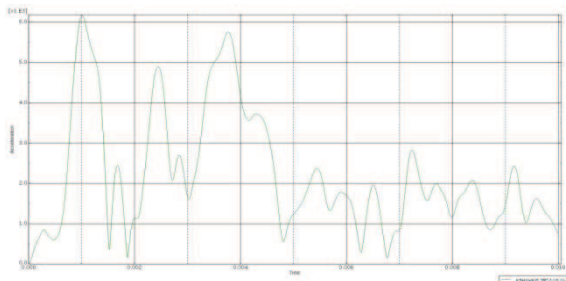

Figure 11. Acceleration received from a simulation of the keel of the explosion front of the bow the ship from a distance of 20 m, depth 15 m, TNT load mass 250 kg

CONCLUSIONS

The results of testing allowed performing simulations of a similar nature to the actual loads of underwater explosions. Virtual model of the hull of the ship responds in a similar manner to the real impacts. Most simulations were performed to calculate or estimate the strength of the hull of plastic deformation. Load model of 2 or 3 bulbs allows assessing the potential occurrence of resonance at any point of the hull. This is important in the design process because the stiffness of the fixing or changing the mass of the foundation, can arrange the marine device from the potential risks coming from the resonance of an underwater explosion.

The next step of research are modeling much more complicate structure of the hull, machinery and other equipments of mine hunter and then solving the problem of resonance between natural frequency of machines and periodical forces coming from first three bulbs effect of underwater detonation.

REFERENCES

[1] Kacprzyk Z., Rakowski G. *Metoda elementów skończonych w mechanice konstrukcji*. Oficyna Wydawnicza Politechniki Warszawskiej, Wyd.2, Warszawa 2005 r. ISBN: 83-7207-589-1.

[2] Szturomski B. *Podstawy Metody Elementów Skończonych*. Wydawnictwo Akademickie AMW, Gdynia 2011, ISBN 978-83-60278-5

[3] Bathe K. J., Wilson E. L. *Numerical method in finite element analysis.* Prentice-Hall, Inc. Englowood Clifts, New Jersey, 1976 r.

[4] Kleiber M. *Metoda elementów skończonych w nieliniowej mechanice kontinuum*. Polska Akademia Nauk, Wyd.1, PWN, Warszawa-Poznań 1985.

[5] Zienkiewicz O. C. *The Finite Element Method in Engineering Science*. McGRAW-HILL, London 1971.

[6] Dobrociński S. *Stabilność rozwiązań zagadnień odporności udarowej konstrukcji*. Biblioteka Problemów Eksploatacji, Akademia Marynarki Wojennej, Gdynia 2000 r., ISBN 83-7204-163-6.

[7] Abaqus 6.10, PDF Documentation, *Theory Manual, Simulia, Dassault Systems*.

[8] Szturomski B.,. Dobrociński S., Flis L. *Analiza wytrzymałościowa konstrukcji pojazdu morskiego obciążonego niekontaktowym wybuchem podwodnym*. Zesz. Nauk. AMW, ROK XLIII NR 2 (150) 2003.

[9] Machowicz M. *Oddziaływanie powietrznej fali uderzeniowej na otoczenie*. ZN Górnictwo i Geoinżynieria, Rok 29, Zeszyt 3, Akademia Górniczo-Hutnicza, Kraków 2005.

[10] Cole R. H. *Underwater Explosions*. Princeton University Press, Princeton 1948.

dr hab. inż. **Andrzej GRZĄDZIELA**
Akademia Marynarki Wojennej
Wydział Mechaniczno - Elektryczny
ul. Śmidowicza 69
81-103 Gdynia
tel. (58) 626 27 24, e-mail
a.grzadziela@amw.gdynia.pl

dr inż. **Bogdan SZTUROMSKI**
Akademia Marynarki Wojennej
Wydział Mechaniczno - Elektryczny
ul. Śmidowicza 69
81-103 Gdynia
tel. (58) 626 27 30, e-mail
b.szturomski@amw.gdynia.pl

mgr inż. **Marcin KLUCZYK**
Akademia Marynarki Wojennej
Wydział Mechaniczno - Elektryczny
ul. Śmidowicza 69
81-103 Gdynia
tel. (58) 626 26 67, e-mail
m.kluczyk@amw.gdynia.pl